PHÂN TÍCH ĐÁP ỨNG ĐỘNG CỦA TẤM FGP SỬ DỤNG PHƯƠNG PHÁP PHẦN TỬ HỮU HẠN

DYNAMIC RESPONSE ANALYSIS OF FGP PLATES USING FINITE ELEMENT FORMULATION

Ngo Van Quang
Faculty of Special Equipments, Le Quy Don Technical University

ABSTRACT

This paper proposes a finite element method (FEM) based on Mindlin plate theory for analyzing the dynamic response of the functionally graded porous (FGP) plate. The FGP materials with two-parameter are the power-law index (k) and the porosity volume fraction (ξ) in two cases of even and uneven porosity. Some numerical results in our work are compared with other published to verify accuracy and reliability of the proposed method. Moreover, the effect of geometric parameters, material properties on the dynamic response of FGP plates is also fully investigated.

Keywords: FEM; Functionally Graded Porous; Dynamic Analysis.

TÓM TẮT

Bài báo này đề xuất phương pháp phần tử hữu hạn (FEM) dựa trên lý thuyết tấm Mindlin để phân tích đáp ứng động của tấm phân loại chức năng có lỗ rỗng (FGP). Vật liệu FGP với hai tham số là chỉ số mũ thể tích (k) và hệ số lỗ rỗng (ξ) trong hai trường hợp phân bố lỗ rỗng đều và không đều. Một số kết quả trong công việc của chúng tôi được so sánh với các kết quả đã công bố trước đây để xác minh tính chính xác và độ tin cậy của phương pháp được đề xuất. Ngoài ra, ảnh hưởng của các thông số hình học, tính chất vật liệu đến đáp ứng động của tấm FGP được thực hiện.

Từ khoá: *Phần tử hữu hạn; Tấm có lỗ rỗng; Phân tích đáp ứng động.*

1. INTRODUCTION

In recent years, the FGP materials have attracted great interest from many researchers over the world. Basically, porosity reduces the stiffness of the structure, however with engineering properties such as lightweight, excellent energy-absorbing capability, great thermal resistant properties, etc, they still have been widely applied in various fields including aerospace, automotive industry, and civil engineering. Some typical works can be summarized as Kim et al. [1] investigated bending, vibration and buckling of the FGP micro-plates using a modified couples stress based on the analytical method. Chen et al. [2] investigated the static bending and buckling of the FGP beams by using the Timoshenko beam theory. Rezaei and Saidi [3], [4] studied the vibration of rectangular and porous-cellular ☞

plates based on an analytical method. The vibration of the FGP shallow shells using an improved Fourier method was examined by Zhao et al. [5]. Recently, Tran et al. [6] studied the dynamic response of FGP plates lying on the EF using smooth-FEM. The FGP materials have many different types, in this paper, the authors use the distribution of porosity as presented in [7].

According to the best of the authors' knowledge, the dynamic response analysis of FGP plates has been not published yet. This motivates us to develop the eight-node quadrilateral (Q8) element combine with Mindlin plate theory to describe the stress-strain and displacement field of FGP plates. The obtained governing equation by using Hamilton's principle. The accuracy and reliability of the present approach are verified by comparing numerical results with other publications. Moreover, the effects of geometry parameters and material properties on the dynamic response of FGP plates are examined.

2. GOVERNING EQUATIONS

2.1. The FGP plate

Let us consider an FGP plate as shown in Fig. 1.

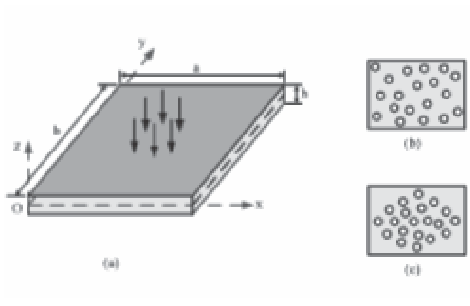

Fig. 1. The FGP plate model.
(a) The FGP plate, (b) Even porosity, (c) Uneven porosity.

The FGP materials with a variation of two constituents and two different distributions of porosity through-thickness are defined by [7]:

Case 1: $$P(\mathrm{z}) = P_m + (P_c - P_m)\left(\frac{z}{h} + 0,5\right)^k - \frac{\xi}{2}(P_c + P_m) \quad (1)$$

Case 2: $$P(\mathrm{z}) = P_m + (P_c - P_m)\left(\frac{z}{h} + 0,5\right)^k - \frac{\xi}{2}(P_c + P_m)\left(1 - \frac{2|z|}{h}\right) \quad (2)$$

Where P is the effective material property. k is the volume fraction index, ξ ($\xi \le 1$) represents the porosity volume fraction. Subscripts m and c denotes the metallic and ceramic constituents, respectively.

2.2. The plate element

In this article, the eight-node quadrilateral plate element is used. Each node has five degrees of freedom (DOF). The nodal displacement vector can be defined by:

$$\mathbf{d}_e = [\mathbf{d}_1^T \quad \mathbf{d}_2^T \quad \mathbf{d}_3^T \quad \mathbf{d}_4^T \quad \mathbf{d}_5^T \quad \mathbf{d}_6^T \quad \mathbf{d}_7^T \quad \mathbf{d}_8^T]^T \quad (9)$$

The displacements at the node i ($i = 1 \div 8$) of element is expressed as

$$\mathbf{d}_i = \left\{u_{0i} \quad v_{0i} \quad w_{0i} \quad \varphi_{xi} \quad \varphi_{yi}\right\} \quad (10)$$

The displacements field in the plate element is interpolated through the displacement node as

$$u_0 = \mathbf{N}_u.\mathbf{d}_e;\ v_0 = \mathbf{N}_v.\mathbf{d}_e;\ w_0 = \mathbf{N}_w.\mathbf{d}_e;\ \varphi_x = \mathbf{N}_{\varphi x}.\mathbf{d}_e;\ \varphi_y = \mathbf{N}_{\varphi y}.\mathbf{d}_e \quad (11)$$

Where $\mathbf{N}_u, \mathbf{N}_v, \mathbf{N}_w, \mathbf{N}_{\varphi x}, \mathbf{N}_{\varphi y}$ are the shape functions.

$$\begin{cases} \mathbf{N}_u = \left[\mathbf{N}_1^{(1)} \quad \mathbf{N}_2^{(1)} \quad \dots \quad \mathbf{N}_7^{(1)} \quad \mathbf{N}_8^{(1)}\right]; \mathbf{N}_v = \left[\mathbf{N}_1^{(2)} \quad \mathbf{N}_2^{(2)} \quad \dots \quad \mathbf{N}_7^{(2)} \quad \mathbf{N}_8^{(2)}\right]; \\ \mathbf{N}_w = \left[\mathbf{N}_1^{(3)} \quad \mathbf{N}_2^{(3)} \quad \dots \quad \mathbf{N}_7^{(3)} \quad \mathbf{N}_8^{(3)}\right]; \\ \mathbf{N}_{\varphi x} = \left[\mathbf{N}_1^{(4)} \quad \mathbf{N}_2^{(4)} \quad \dots \quad \mathbf{N}_7^{(4)} \quad \mathbf{N}_8^{(4)}\right]; \mathbf{N}_{\varphi y} = \left[\mathbf{N}_1^{(5)} \quad \mathbf{N}_2^{(5)} \quad \dots \quad \mathbf{N}_7^{(5)} \quad \mathbf{N}_8^{(5)}\right]. \end{cases} \quad (12)$$

The element stiffness matrix is determined by

$$\mathbf{K}_e = \mathbf{K}_e^b + \mathbf{K}_e^s \quad (13)$$

With $\mathbf{K}_e^b, \mathbf{K}_e^s$ are the bending, shear element stiffness matrices, respectively.
in which

$$\mathbf{K}_e^b = \int_{S_e} \left(\left[\mathbf{B}_1^T \quad \mathbf{B}_2^T\right] \begin{bmatrix} \mathbf{A} & \mathbf{B} \\ \mathbf{B} & \mathbf{H} \end{bmatrix} \begin{bmatrix} \mathbf{B}_1 \\ \mathbf{B}_2 \end{bmatrix} \right) dxdy \quad (14)$$

$$\mathbf{K}_e^s = \int_{S_e} \mathbf{B}_3^T \mathbf{A}^s \mathbf{B}_3 dxdy \quad (15)$$

Where

$$\mathbf{B}_1 = \begin{bmatrix} \mathbf{N}_{u,x} \\ \mathbf{N}_{v,y} \\ \mathbf{N}_{u,x} + \mathbf{N}_{v,y} \end{bmatrix}; \mathbf{B}_2 = \begin{bmatrix} \mathbf{N}_{\varphi x,x} \\ \mathbf{N}_{\varphi y,y} \\ \mathbf{N}_{\varphi x,y} + \mathbf{N}_{\varphi y,x} \end{bmatrix}; \mathbf{B}_3 = \begin{bmatrix} \mathbf{N}_{w,x} + \mathbf{N}_{\varphi x} \\ \mathbf{N}_{w,y} + \mathbf{N}_{\varphi y} \end{bmatrix} \quad (16)$$

The element mass matrix is given by

$$\mathbf{M}_e = \int_{S_e} \mathbf{N}^T \mathbf{m}_p \mathbf{N} dxdy \quad (17)$$

in which

$$\mathbf{N} = \left[\mathbf{N}_u^T \quad \mathbf{N}_v^T \quad \mathbf{N}_w^T \quad \mathbf{N}_{\theta x}^T \quad \mathbf{N}_{\theta y}^T\right] \quad (18)$$

$$\mathbf{m}_p = \begin{bmatrix} I_1 & 0 & 0 & I_2 & 0 \\ & I_1 & 0 & 0 & I_2 \\ & & I_1 & 0 & 0 \\ & & & I_3 & 0 \\ & & & & I_3 \end{bmatrix} \quad (19)$$

with $(I_1, I_2, I_3) = \int_{-h/2}^{h/2} \rho\,(1, z, z^2) dz$.

The element force vector is:

$$\mathbf{F}_e = \int_{S_e} \mathbf{N}^T \mathbf{P} dxdy \quad (20)$$

in there

$$\mathbf{P} = [0 \quad 0 \quad p \quad 0 \quad 0]^T \quad (21)$$

Hamilton's principle leads to the motion equation of FGP plates as follows:

$$\mathbf{M}.\ddot{\mathbf{d}} + \mathbf{K}.\mathbf{d} = \mathbf{F} \quad (22)$$

Where $\mathbf{M}, \mathbf{K}, \mathbf{F}, \mathbf{d}$ are the global mass matrix, the global stiffness matrix, the global force vector, and the global displacement vector. If structural damping is included, the equation of motion of plates is:

$$\mathbf{M}.\ddot{\mathbf{d}} + \mathbf{C}.\dot{\mathbf{d}} + \mathbf{K}.\mathbf{d} = \mathbf{F} \quad (23)$$

In which $\mathbf{C} = \alpha\mathbf{M} + \beta\mathbf{K}$ the global structural resistance matrix with α, β are Rayleigh resistance coefficients, which are determined by the resistance ratio ζ and the first two frequencies (ω_1, ω_2) [9]. In order to solve this equation, we use the Newmark method [9].

3. VERIFICATION PROBLEM

In this sction, the fully clamped (CCCC) homogeneous plate with parameters a = b = 1m, h = a/10, E = 300 GPa, ρ = 2800Kg/m^3 and υ=0.3 is considered. The plate is subjected to distribution sudden load p_0 = 10kPa. The non-dimensional deflection is given by the formula $w^* = \dfrac{100Eh^3}{12p_0a^4(1-\upsilon^2)}w$. The deflection response of the midpoint of the plate is shown in Fig. 2, (integral time is 5ms, and acting time of load is 2ms). Observing this figure, it can ☞

be seen that the deflection response of the plate center point is compared to [10] which uses Meshless Petrov-Galerkin (MLPG) method is similar in both shape and value. From the above examples, it can be concluded that the author's formula and program ensure accuracy and reliability.

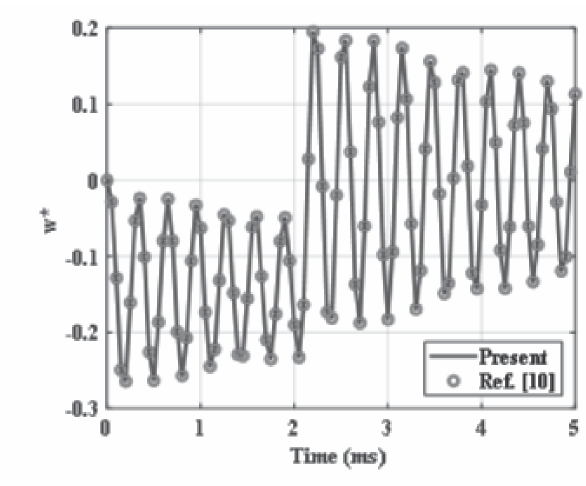

Fig. 2. The deflection response of the plate center point over time.

4. NUMERICAL RESULTS

In this section, we consider an FGP plate with material properties are listed in Table 2. Fig. 3 shows the first four-mode shapes of FGP (Case 1) square plate has geometric dimensions a = b =1 m, h = a/10 and the remaining material parameters k = 1, ξ = 0.2. It can be observed that the second and third mode shapes are similar to each other. This is suitable for the symmetrical plates under the same supported conditions. It should note that the dimensionless parameters of the FGP plates are introduced by the following formulations:

$$w^* = \frac{10E_m h^3}{q_0 a^4} w;\ \Omega = 10\omega h\sqrt{\frac{\rho_m}{E_m}} \qquad (24)$$

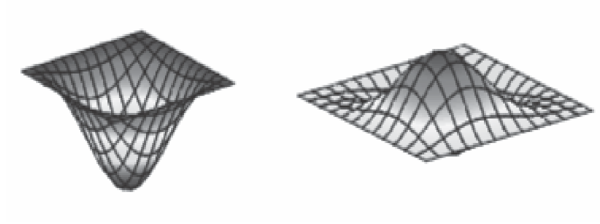

(a) Mode 1 (b) Mode 2

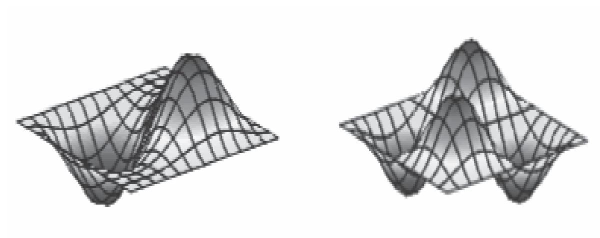

(c) Mode 3 (d) Mode 4

Fig. 3. The first four mode shapes of the SSSS FGP (Case 1) plate.

(a) 1st mode, Ω_1 = 0.8237; (b) 2nd mode, Ω_2 = 1.9794; (c) 3rd mode, Ω_3 = 1.9794; (d) 4th mode, Ω_4 = 3.0546.

Next, authors consider a (Al_2O_3/Al) FGP nanoplate with geometric dimensions a = b =1 m, h = a/25. The FGP nanoplate is subjected to a uniform load p(t) over time as follows:

$$p(t) = q_0.F(t);\quad F(t) = \begin{cases} 1 - \dfrac{t}{\tau_{hd}} & \left(0 \le t \le \tau_{hd}\right) \\ 0 & otherwise \end{cases} \qquad (25)$$

With q_0 is is uniformly distributed load and $\tau_{hd} = 0.02$ (s). The damping ratio in the below examples are chosen as $\zeta = 0.05$.

Fig. 4 presents the effect of power-law index k on the displacement response of the SSSS FGP (Case 1) plate with porosity volume fraction $\xi = 0.2$. It can be observed that power-law index *k* increase makes reduce stiffness of the plate leads to displacement increase. Besides, rich-metal plate's stiffness is smaller than rich-ceramic plate's stiffness.

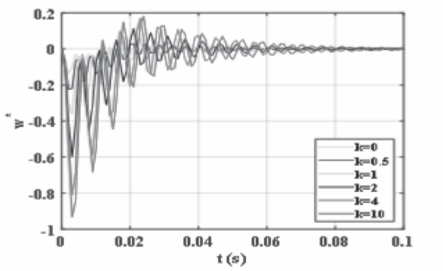

Fig. 4. The displacement response of the SSSS FGP (Case 1) plate.

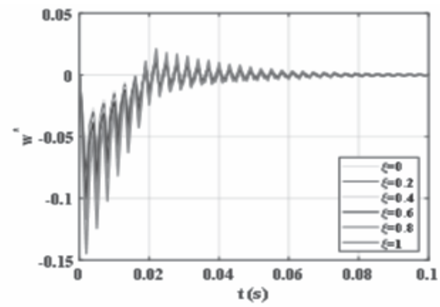

Fig. 5. The displacement response of the CCCC FGP (Case 2) plate.

Finally, Fig. 5 displays the influence of porosity volume fraction on the displacement response of the CCCC FGP (Case 2) plate with power-law index k = 1. It can be observed that porosity volume fraction ξ increase leads to plate's stiffness reduce, therefore displacement response of the plates increase. It can also be seen that, after the time of application of the load, the displacement response of the plate decreases gradually due to the consideration of the structural resistance.

5. CONCLUSIONS

In this article, the dynamic analysis of the FGP plate is studied by using the FEM based on Mindlin plate theory. The obtained numerical results of the present approach are compared to other available solutions to verify accuracy and reliability. From the proposed formulation and the numerical results, we can withdraw some following points:

- The mechanical parameters as well as the porosity distribution of the FG material effect significantly the dynamic response of FGP plates. Specifically, the power-law index k and porosity volume fraction ξ make decrease the stiffness of plates.

- Vibrations are reduced after the time the load is applied due to the consideration of structural resistance.

- Numerical results in the present work are useful for the calculation, designing of FGP plates in engineering and technologies.❖

References:

[1]. Jinseok Kim, Krzysztof Kamil Żur, J.N. *Reddy, Bending, free vibration, and buckling of modified couples stress-based functionally graded porous micro-plates,* Composite Structures (2019), 209, 879-888.

[2]. Chen D, Yang J, Kitipornchai S. *Elastic buckling and static bending of shear deformable functionally graded porous beam*. Compos Struct. 2015;133:54-61.

[3]. Rezaei AS, Saidi AR. *Application of Carrera Unified Formulation to study the effect of porosity on natural frequencies of thick porous–cellular plates.* Compos Part B-Eng. 2016;91:361-70.

[4]. Rezaei AS, Saidi AR. *Exact solution for free vibration of thick rectangular plates made of porous materials*. Compos Struct. 2015;134:1051-60.

[5]. Zhao J, Xie F, Wang A, Shuai C, Tang J, Wang Q. *A unified solution for the vibration analysis of functionally graded porous (FGP) shallow shells with general boundary conditions.* Compos Part B-Eng. 2018.

[6]. T.T. Tran, Q.-H. Pham, T. Nguyen-Thoi, *Dynamic analysis of functionally graded porous plates resting on elastic foundation taking into mass subjected to moving loads using an edge-based smoothed finite element method*, Shock and Vibration, 2020 (2020).

[7]. S. Narendar, S. Gopalakrishnan S. *Nonlocal continuum mechanics based ultrasonic flexural wave dispersion characteristics of a monolayer graphene embedded in polymer matrix.* Composites Part B: Engineering, 43, (8), (2012), pp. 3096-3103.

[8]. Reddy JN. *Mechanics of laminated composite plates and shells: theory and analysis:* CRC press; 2003.

[9]. Wolf J. *Dynamic SoilStructure Interaction.* PrenticeHall. Inc., Englewood Cliffs, New Jersey. 1985.

[10]. Qian, L.F. *Free and Forced Vibrations of Thick Rectangular Plates using Higher-Order Sheara and Normal Deformable Plate Theory and Meshless Petrov-Galerkin (MLPG) Method.* CMES 2003, 5, 519–534.